

1 CODEC enables ‘single duplex’ sequencing

2 Jin H. Bae[†],¹ Ruolin Liu[†],¹ Erica Nguyen,¹ Justin Rhoades,¹ Timothy Blewett,¹ Kan Xiong,¹ Douglas Shea,¹ Gregory Gydush,¹
3 Shervin Tabrizi,^{1,2,3} Zhenyi An,¹ Sahil Patel,¹ G. Mike Makrigiorgos,⁴ Todd R. Golub,¹ and Viktor A. Adalsteinsson*¹

4 ¹*Broad Institute of MIT and Harvard, Cambridge, Massachusetts, USA*

5 ²*Koch Institute for Integrative Cancer Research at MIT, Cambridge, Massachusetts, USA*

6 ³*Harvard Radiation Oncology Program, Boston, Massachusetts, USA*

7 ⁴*Dana-Farber Cancer Institute, Boston, Massachusetts, USA*

8 [†]*Equal contribution*

9 ^{*}*Correspondence should be addressed to V.A.A. (email: viktor@broadinstitute.org)*

10 *(Dated: June 11, 2021)*

Abstract

11 Detecting mutations as rare as a single molecule is crucial in many fields such as cancer diagnostics
12 and aging research but remains challenging. Third generation sequencers can read a double-stranded
13 DNA molecule (a ‘single duplex’) in whole to identify true mutations on both strands apart from false
14 mutations on either strand but with limited accuracy and throughput. Although next generation
15 sequencing (NGS) can track dissociated strands with Duplex Sequencing, the need to sequence each
16 strand independently severely diminishes its throughput. Here, we developed a hybrid method called
17 Concatenating Original Duplex for Error Correction (CODEC) that combines the massively parallel
18 nature of NGS with the single-molecule capability of third generation sequencing. CODEC physically
19 links both strands to enable NGS to sequence a single duplex with a single read pair. By comparing
20 CODEC and Duplex Sequencing, we showed that CODEC achieved a similar error rate (10^{-6}) with
21 100 times fewer reads and conferred ‘single duplex’ resolution to most major NGS workflows.

Introduction

22 Discovering extremely low-level mutations as rare as within
23 a single double-stranded DNA molecule (a ‘single duplex’)
24 is crucial to finding diagnostic[1, 2], predictive[3, 4], and
25 prognostic[5, 6] biomarkers, understanding cancer evolution[7,
26 8] and somatic mosaicism[9, 10], and studying infectious
27 diseases[11, 12] and aging[13, 14]. Third generation sequencing
28 technologies (e.g., PacBio, Oxford Nanopore Technologies)
29 in principle make it possible to sequence each single DNA
30 duplex in whole to resolve true mutations on both strands
31 apart from false mutations on either strand, but, in practice,
32 lack the required accuracy and throughput[15, 16]. Next
33 generation sequencing (NGS), on the other hand, continues
34 to offer superior read accuracy and throughput[17], but is not
35 configured to sequence single duplexes—at least not without
36 severely compromising its throughput or utility.

38 NGS affords high throughput by reading short, clonally
39 amplified DNA fragments in massively parallel fluorescence
40 analysis. Yet, its accuracy is limited by the need to dissociate
41 Watson and Crick strands of each DNA duplex. Without
42 a complementary strand for comparison, errors introduced
43 on either strand due to base damage[18], PCR[19], and
44 sequencing[20] can be disguised as real mutations (Fig. 1a).
45 While it is possible to use unique molecular identifiers (UMIs)
46 to separately track both strands of each DNA molecule and
47 compare their sequences to detect true mutations on both
48 strands of each duplex[21, 22], it does not solve the underlying
49 limitation of NGS: duplex dissociation. For example,
50 Duplex Sequencing[23] tags double-stranded UMIs on each
51 original duplex to trace them back after PCR and NGS. By
52 forming a duplex consensus between reads assigned to the
53 Watson and Crick strands of each original duplex, Duplex
54 Sequencing achieves 1,000-fold or higher accuracy (error rate
55 below 10^{-6}) and can thus resolve true mutations within single
56 DNA duplexes. However, recovering both strands among up
57 to 10 billion other strands on an NGS flow cell (e.g., Illumina

58 NovaSeq) requires 100-fold excess reads[24], which invariably
59 diminishes the throughput of NGS and severely limits its
60 applicability.

61 To date, a few methods have sought to overcome the high
62 inefficiency of Duplex Sequencing. Duplex Proximity Sequencing
63 (Pro-Seq)[25] uses a polyethylene glycol linker to link 5'-
64 ends of an original Watson strand and a copied Crick strand
65 of a duplex to avoid hairpin formation for whole-genome sequencing
66 (WGS). However, concatenating two strands with
67 the opposite directions blocks DNA amplification which is
68 necessary for most applications. CypherSeq[26] generates a
69 circularized duplex followed by rolling circle amplification,
70 but the lack of asymmetry between the two strands obscures
71 whether both strands were actually sequenced. Some technologies
72 such as o2n-seq[27] and Circle Sequencing[28] are
73 compatible with PCR but only link a single strand of each
74 duplex and thus, lack the ability to create a duplex consensus.
75 BotSeqS[29, 30] uses dilution instead of linking to increase
76 the chance of recovering both strands, but by doing so it only
77 sequences 0.001% of the input DNA. Despite the need for sequencing
78 single duplexes with high accuracy and throughput,
79 there has been no such method with universal applicability.
80 We thus reasoned that linking the information of both strands
81 before dissociation could make NGS capable of reading single
82 DNA duplexes with high accuracy and throughput.

83 Here, we developed a method that combines the massively
84 parallel nature of NGS and the single-molecule capability
85 of third generation sequencing to sequence both strands of
86 each DNA duplex with single read pairs. In this hybrid
87 approach called Concatenating Original Duplex for Error
88 Correction (CODEC), each molecule becomes self-sufficient
89 for forming a duplex consensus via NGS (Fig. 1a). By
90 using the opposite strand as a template for extension instead
91 of directly linking them, CODEC physically concatenates
92 the sequence information of Watson and Crick strands into
93 a single strand without forming a strong hairpin structure
94 (Fig. 1b). Any differences between concatenated sequences

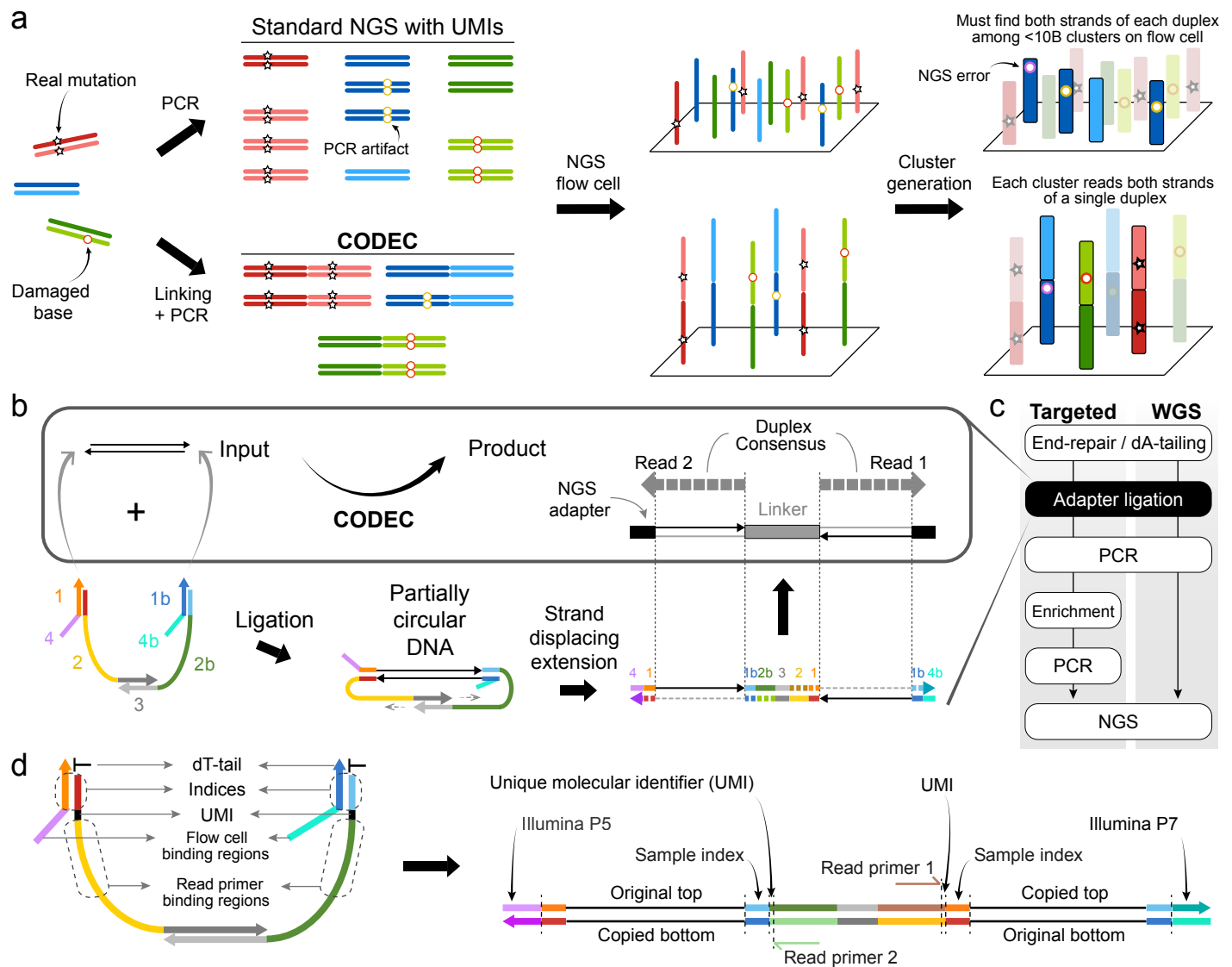


FIG. 1. Overview of Concatenating Original Duplex for Error Correction (CODEC). (a) Standard NGS workflows involve dissociation of DNA duplex, which loses the intrinsic property of DNA that encodes genetic information twice. Both strands of a duplex can be tracked through unique molecular identifiers (UMIs) to identify false mutations caused by base damage, PCR, and NGS errors, but finding them among <10 billion other strands costs throughput, highlighted by blue clusters. CODEC physically links each duplex before dissociation, ensuring each library molecule retains information of both strands. (b) CODEC links the sequence information of an original duplex into a single strand. As a result, each pair of NGS reads becomes self-sufficient for forming a duplex consensus (box). It utilizes the adapter complex instead of a duplex adapter for ligation, followed by strand displacing extension. (c) CODEC modifies the ligation step of ligation-based NGS workflows. (d) CODEC adapter complex is prepackaged with all of the components needed for Illumina NGS. Unlike standard NGS libraries, CODEC reads outward to sequence a UMI, an index, and an insert together. No indexed primers are required as indices and flow cell binding regions (P5 and P7) are added by the ligation.

would indicate either non-canonical base pairing created by nucleobase damage or an alteration confined to one strand of the original DNA duplex, or an error introduced during PCR amplification or sequencing. We tested CODEC with different sample types and NGS workflows, and confirmed that it suppressed both single nucleotide variants (SNV) and indel errors as accurately as Duplex Sequencing but with 100-fold fewer reads, thereby conferring 'single duplex' resolution to NGS.

Results

CODEC adapter complex and workflow. The CODEC structure can be built by a streamlined workflow using a commercial ligation-based NGS preparation kit and CODEC adapter complex. First, a typical duplex adapter was replaced with the adapter complex consisting of four oligonucleotides,

containing all elements required for NGS. We rationally designed double-stranded segments of the adapter to hold the whole complex based on DNA hybridization thermodynamics (**Supplementary Figure S1a**) and introduced single-stranded segments to mitigate bending stiffness of rigid double helix (**Supplementary Figure S1b**). After adapter ligation closes both ends of an input molecule, strand displacing extension initiates at remaining 3'-ends to elongate each strand by using the opposite strand as a template. The resulting structure is two original strands concatenated with the CODEC linker in the middle and NGS adapters on both sides. The molecular process depicted in **Fig. 1b** is integrated into the adapter ligation step of commercial NGS library construction kits (**Fig. 1c**).

To fully utilize the concatenated structure, we also relo-

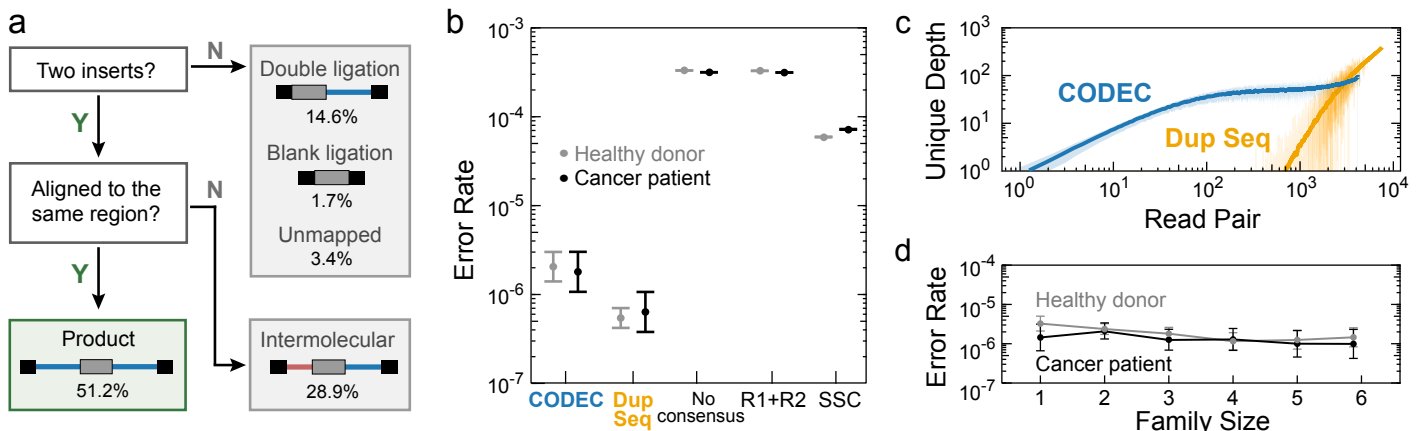


FIG. 2. Proof-of-concept. (a) Ratios of the correct CODEC product and byproducts which have been named after how they were likely created. (b) Error rates of CODEC, Duplex Sequencing, and other consensus methods including typical paired-end read (R1+R2) and single strand consensus (SSC). Target enrichment with a pan-cancer gene panel was performed on cell-free DNA (cfDNA) of two individuals. Error bars indicate 95% binomial confidence intervals. (c) Recovery of unique original duplexes per captured region in healthy donor cfDNA against the amount of sequencing. Solid lines show moving averages and shades indicate standard deviations. (d) CODEC error rates at each family size, which is the number of raw reads with the same UMI and start-stop positions.

125 cated the NGS library components (Fig. 1d). In contrast to 126 the conventional Illumina structure with the NGS read primer 127 binding sites on the outer side, we moved the binding sites 128 to the CODEC linker in the middle and sequenced outward 129 to prevent reading molecules without the linker (Supple- 130 mentary Figure S1c). Having the binding sites at conven- 131 tional locations had resulted in poor Quality Scores, which 132 we attributed to template hopping in cluster amplification 133 (Supplementary Figure S2a), whereas moving the bind- 134 ing sites to the linker overcame this issue (Supplementary 135 Figure S2b). Sample indices, which are typically located 136 outer to the read primer binding sites and read separately 137 from the inserts, were moved right next to the inserts. By 138 adding the indices during adapter ligation and reading them 139 with the inserts in a single step, CODEC suppressed index 140 hopping even better than the gold standard of using unique 141 dual indices[31, 32] (0.056% vs. 0.16%). We designed sets 142 of 4 sample indices that collectively have all four bases at 143 every position to ensure high base diversity for proper clus- 144 ter identification, phasing correction, and chastity filtration 145 (Supplementary Figure S3). Because indexed primers 146 were no longer needed, we were able to include Illumina P5 147 and P7 segments in the adapter complex and use them as 148 universal primer binding regions.

149 **Proof-of-concept.** We first confirmed that the CODEC 150 workflow could create the intended NGS library structure 151 by converting fragmented human genomic DNA (gDNA) 152 from peripheral blood mononuclear cells into a CODEC- 153 NGS library and sequencing it. Due to the novel structure of 154 CODEC reads, we created a user-friendly analysis pipeline 155 called CODECsuite to process the data (see Methods). We 156 found that more than half of the reads showed the correct 157 structure (Fig. 2a). Meanwhile, the major byproducts ap- 158 peared to have been created when an input duplex was either 159 ligated to two different adapter complexes (“double ligation”) 160 or no adapter complex (“blank ligation”), or when strand 161 displacing extension occurred between two ligated products 162 (“intermolecular”) (Supplementary Figure S4). Yet, al- 163 most 90% of byproducts still retained information on one 164 side of a duplex just like standard NGS, suggesting that the

165 byproducts may still yield useful data.

166 We next explored whether the fragments with the correct 167 CODEC structure could provide comparable error rates to 168 Duplex Sequencing using significantly fewer reads. To assess 169 this, we performed a head-to-head comparison. Because 170 Duplex Sequencing requires high sequencing depth per locus, 171 we ran target enrichment with a pan-cancer panel on NGS 172 libraries prepared with each method, built from 20 ng cell-free 173 DNA (cfDNA) from a cancer patient and a healthy donor. 174 We found that the mean CODEC error rate of two individuals 175 (1.9×10^{-6}) was similar to that of Duplex Sequencing (5.9×10^{-7}) (Fig. 2b) with no statistically significant difference in 177 sequence contexts of errors except for C:G>T:A in a healthy 178 donor (Supplementary Figure S5a), which we believe 179 could be resolved using an improved end-repair method[30, 33] 180 (Supplementary Figure S5b). Additionally, when error 181 rates were plotted as a function of distance from either end 182 of a fragment, we saw elevated error rates from CODEC and 183 Duplex Sequencing data toward the fragment ends of duplex 184 consensus, consistent with prior reports of error propagation 185 in end-repair[30, 33] (Supplementary Figure S6). This 186 observation reassures that reading a single CODEC fragment 187 is equivalent to reading two Duplex Sequencing fragments 188 from each strand and affirms the need to trim 12 base pairs 189 (bp) from both ends of each original DNA duplex in silico[24].

190 To further confirm that the error suppression potential of 191 CODEC is uniquely enabled by reading both strands of the 192 original DNA duplex together, as opposed to simply forming 193 a consensus of forward and reverse reads, we then compared 194 error rates of three additional methods from the same NGS 195 data: no consensus, paired-end reads consensus (R1+R2, col- 196 lapses read 1 and read 2), and single strand consensus (SSC, 197 collapses reads from the same original strand). Interestingly, 198 the error rate gap between the no consensus and R1+R2 199 was negligible (Fig. 2b), suggesting that many errors are 200 physically present in NGS library molecules, and could have 201 been introduced during library amplification, or when each 202 library molecule undergoes bridge amplification for cluster 203 generation (Fig. 1a). Although SSC was more accurate than 204 R1+R2 and the no consensus reads, without a consensus of

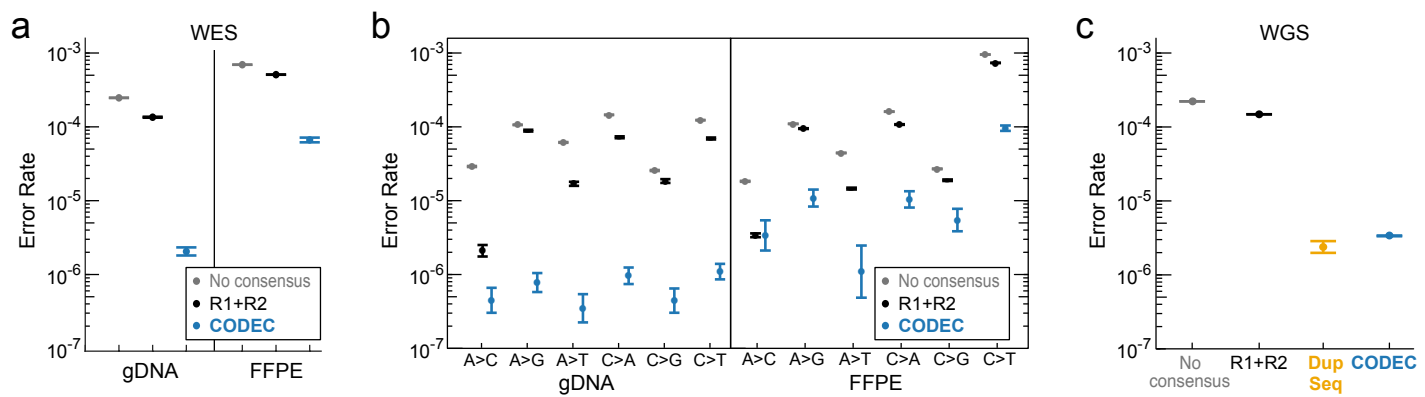


FIG. 3. Error rates of whole-exome sequencing (WES) and whole-genome sequencing (WGS). (a) Error rates of CODEC on formalin-fixed paraffin-embedded (FFPE) and matching normal samples of a cancer patient. (b) Errors in (a) broken down by sequence context. (c) Error rates of WGS with Duplex Sequencing and CODEC performed side by side.

Watson and Crick strands, its error rate was 23-fold higher than that of CODEC. The fact that reading the same strand multiple times does not contribute as much as duplex consensus implies the intrinsic limitation of other sequencing technologies[27, 28].

We next explored the number of reads required to uncover the same number of unique DNA duplexes. When we used UMIs as well as start and stop mapping positions of each molecule to collapse all reads to unique original duplexes, we found that Duplex Sequencing could not start reassembling duplexes until receiving 700 reads (Fig. 2c). In contrast, CODEC started to reassemble 350-fold earlier. The gap between required reads was maximized when recovering a smaller number of duplexes, suggesting that CODEC could be uniquely capable of sequencing broad genomic regions with shallow depth. Notably, even a single paired-end read of CODEC was highly accurate (Fig. 2d), as each CODEC read is self-sufficient to form a duplex consensus. Our results suggest that CODEC confers the accuracy of duplex sequencing from single paired-end reads and thus sequences more DNA duplexes using substantially fewer reads.

CODEC confers the accuracy of duplex sequencing to WGS and WES. We next sought to determine whether CODEC could enable human whole-exome and whole-genome ‘duplex’ sequencing, which would otherwise be impractical due to high cost. To assess this, we applied CODEC whole-exome sequencing (WES) to gDNA and formalin-fixed paraffin-embedded (FFPE) samples from a cancer patient, whose samples had been tested in our prior publication[24]. We found that CODEC reduced the sequencing error rates of both samples, with 100-fold improvement for gDNA (Fig. 3a). Analyzing the sequence context of the errors revealed that CODEC improved accuracy across all types of SNV (Fig. 3b), suggesting that the capability of CODEC to suppress errors is not limited to specific contexts. Of note, there were more C>T errors in FFPE samples due to deamination artifacts[34], which we believe could be resolved with improved end-repair methods[30, 33].

Next, we applied CODEC and Duplex Sequencing to WGS of the pilot genome NA12878 of the Genome in a Bottle Consortium (GIAB)[35]. For a fair comparison, we assigned the same amount of sequencing to each method although Duplex Sequencing could not recover many unique duplexes. The error rates of both Duplex Sequencing (2.38×10^{-6}) and

CODEC (3.37×10^{-6}) were much lower than that of the no consensus reads (2.2×10^{-4}) or R1+R2 (1.48×10^{-4}) (Fig. 3c). This result confirms that CODEC is as accurate as Duplex Sequencing under the same conditions. The error rates of each sequence context showed that CODEC has a similar error profile to Duplex Sequencing (Supplementary Figure S7).

Depth of coverage analysis for WGS further demonstrated that CODEC achieved 160-fold greater unique duplex depth than Duplex Sequencing. On the GIAB v3.3.2 hg19 high confidence genomic region (2.6B bases), CODEC had a mean unique duplex depth of 3.96 with 320M raw reads, whereas Duplex Sequencing had only 0.025 mean depth even with 35% more raw read output (431M reads), because most reads did not find their matching strand of the original duplex (Fig. 4a). Thus, we concluded that Duplex Sequencing is not appropriate for WGS and treated Duplex Sequencing WGS data as standard WGS data without generating duplex consensus after this point. In contrast, CODEC covered each base with four unique duplexes on average, confirming the strength of resolving single duplexes.

CODEC pushes the frontiers in secondary analysis applications. Achieving the error rate of Duplex Sequencing in WGS/WES gives CODEC the ability to push the limits of many secondary analysis applications. One such application is benchmarking the whole genome small germline variant calling (SNV + indel). To test the potential of CODEC at low coverage as implied in Figure 2c, we compared CODEC data of the aforementioned NA12878 sample against standard NGS (R1+R2) at coverages ranging from 1x to 10x, while acknowledging that state-of-the-art germline calling usually requires 30x depth. GATK4 was used for variant calling and followed by the GIAB best practice for benchmarking small germline variants[35]. CODEC showed 90% fewer false positives (FP) than standard WGS with R1+R2 at a cost of 5% higher false negatives (FN) across all downsampled depths (Fig. 4b, Supplementary Table S1). By downsampling NGS data, we also observed how FP and FN are affected by the depth. The lower level of FP in CODEC was the expected result, considering its lower error rate. Its FN levels were slightly higher than that of standard WGS, probably because the lower library conversion efficiency resulted in higher duplication rate, but the difference between FN rates of CODEC and standard WGS became smaller as the cov-

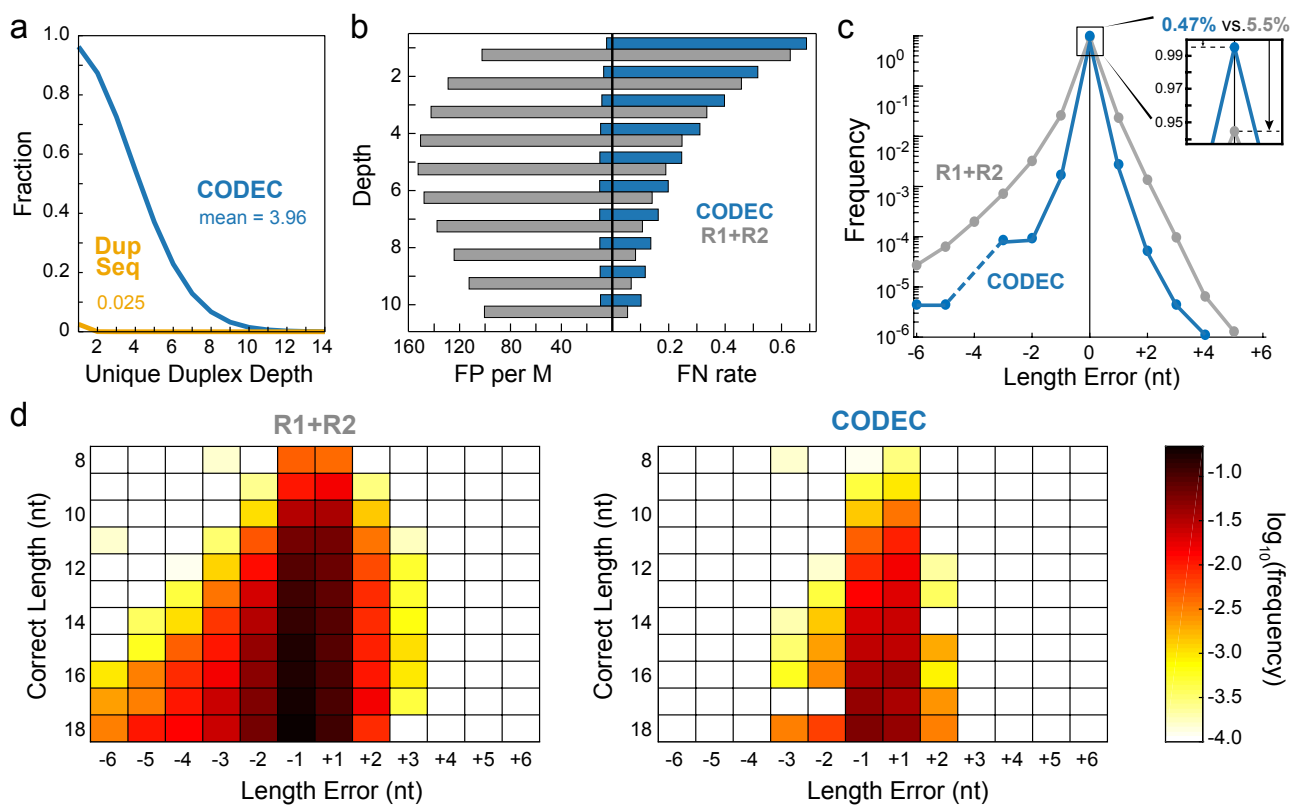


FIG. 4. In-depth comparison of WGS results. (a) Fractions of each unique duplex depth of CODEC and Duplex Sequencing. (b) False positives and false negatives of CODEC and R1+R2 when downsampled to lower depths. (c) Summarized indel error frequency at mononucleotide microsatellites. (d) Indel error frequency at mononucleotide microsatellites with different lengths from 8 to 18 nucleotides.

erage decreased. Meanwhile, the advantage of having low FP became more significant at the lower coverage, implying that applications with shallow depth could benefit more from using CODEC.

Considering CODEC's performance for indel detection at low coverage, we thought that CODEC could improve the sequencing accuracy of microsatellites (MS), which are well-known mutation hot spots. Indeed, when the reference sequences of the MS in NA12878 were compared between CODEC and standard NGS results, CODEC showed lower frequencies of both insertion and deletion errors than standard WGS at mononucleotide MS from 8 to 18 nucleotides (Fig. 4c). The ratio of CODEC reads with incorrect MS lengths was 0.47%, which was 12 times lower than that of standard WGS. Such lower frequencies were consistently observed across mononucleotide MS of varied lengths (Fig. 4d). These findings imply that CODEC could be used to read the repeat numbers/copy numbers of MS sites for detecting microsatellite instability (MSI). MSI has been shown to be a predictive marker of response to cancer immunotherapy but remains challenging to detect at low frequency such as from liquid biopsy samples[36]. Tracing mutations in MS is also useful for tracing cell lineages and evolution[37]. The improvements in the secondary applications we have shown highlight what CODEC could enable by sequencing a single duplex within each NGS cluster.

Discussion

By physically linking both strands of each DNA duplex, CODEC enables each NGS cluster to have single duplex resolution like third generation sequencers. Unlike Duplex

Sequencing which requires dissociating duplexes and recovering them back to form a duplex consensus, CODEC distinguishes real mutations from errors with similarly high accuracy but with 100-fold fewer reads. We first showed the proof-of-concept of our approach using cfDNA enriched by a pan-cancer panel, followed by testing its consistency across other major NGS workflows (e.g., WES and WGS) and sample types (e.g., FFPE and germline DNA). To present more uses of CODEC, we also showed that it suppressed FP especially at shallow sequencing depth and reduced indel errors at MS sites.

In a head-to-head comparison, we showed that CODEC is as accurate as Duplex Sequencing but with a much lower sequencing requirement, which has been a major limitation of Duplex Sequencing. Because an error rate is affected by multiple factors other than a sequencing technology itself, any direct comparison requires everything else to be the same. We used the same experimental and computational protocols whenever applicable, including input samples and mass, reagents, target regions, definition of an error, and analysis pipelines for precise comparison.

Because CODEC redefines standard NGS with a novel molecular structure, there may still be room for improvement in its use with target selection protocols including hybrid capture, multiplexed amplicon, and mutation enrichment sequencing[38]. We are also working to improve CODEC's conversion efficiency. The CODEC adapter complex is attached through two consecutive ligations: a bimolecular ligation followed by a unimolecular ligation. Unlike typical bimolecular adapter ligation where increasing adapter concentration also increases conversion efficiency, unimolecular

354 ligation could be less favorable when the adapter concentra-
355 tion is too high. Consequently, the current version of CODEC
356 adapter complex needs balancing between two ligations. We
357 are currently developing another version of CODEC that
358 circumvents two consecutive ligations.

359 Although conventional end-repair/dA-tailing of a commer-
360 cial kit was used throughout this work, the accuracy can be
361 further improved if a new end-repair method is adopted be-
362 fore CODEC. Recent studies[30, 33] have reported that base
363 damage on overhangs and single-stranded breaks of original
364 DNA duplexes can lead errors on one strand to be copied to
365 both strands. It was also indirectly observed in this work that
366 error rates were generally higher toward the ends of DNA
367 fragments (Supplementary Figure S6). While such errors
368 appear on duplex consensus and result in false mutations,
369 new end-repair methods prevent the error propagation, and
370 we believe that even higher accuracy will be attainable when
371 CODEC is combined with new end-repair methods[30, 33].

372 Reading a single CODEC fragment is equivalent to reading
373 both strands of an original duplex, which eliminates the need
374 to read the same locus multiple times. The low error rate
375 of CODEC at 1x read depth opens possibilities for various
376 applications across fields from diagnostics to bioinformatics.
377 One example is discovering rare somatic mutations with a
378 limited number of reads, which has a higher chance of finding
379 a true mutation when the error rate gets lower[39]. Another
380 example is shotgun metagenomic sequencing for microbiome
381 analysis, where suppressing false SNVs with CODEC would
382 prevent incorrect taxonomic classifications and inaccurate
383 evaluation of microbial diversity[40]. In de novo assembly,
384 lower error rates contribute to more contiguous assembly
385 in de Bruijn graph paradigm and faster process in overlap-
386 layout-consensus paradigm[41].

387 In summary, CODEC transforms standard NGS instru-
388 ments into massively parallel ‘single duplex’ sequencers by
389 concatenating both strands of each original DNA duplex.
390 This strategy enables SNV and indel detection as accurate
391 as Duplex Sequencing, even in cases where Duplex Sequenc-
392 ing is not possible due to low throughput. We thus believe
393 that CODEC could be broadly enabling for many important
394 biomedical applications such as detecting early-stage cancer
395 or minimal residual disease from liquid biopsies, clinically
396 actionable mutations from liquid or tumor biopsies, clonal
397 hematopoiesis of indeterminate potential (CHIP) from blood
398 samples, somatic mosaicism in normal tissue samples, and
399 beyond.

400 Methods

401 **DNA samples and oligonucleotides.** Cell-free DNA of patient 315
402 from cohort 05-246 and both FFPE and gDNA of patient 95 from cohort
403 05-055 were from another study[24]. NA12878 was purchased from
404 Coriell. All samples were stored in low TE buffer (10 mM Tris-HCl, 0.1
405 mM EDTA, pH 8) and were fragmented by Covaris ultrasonicator to have
406 a mean size of 150 bp except cfDNA. All oligonucleotides for CODEC
407 were synthesized by Integrated DNA Technologies (IDT) and went
408 through PAGE purification (See **Supplementary Table S2** for their
409 sequences). The adapter for Duplex Sequencing was custom-ordered for
410 the Broad Institute by IDT.

411 **CODEC.** The CODEC adapter complex was prepared by diluting four
412 100 μ M oligonucleotides to 5 μ M with low TE buffer and 100 mM NaCl,
413 followed by heating at 85 °C for 3 minutes, cooling with -1 °C/min to
414 20 °C, and incubating at room temperature for 12 hours. Mastercycler
415 X50 (Eppendorf) and MAXYMum Recovery PCR tubes (Axygen) were

416 used for the annealing. The annealed adapter complex was kept at -20
417 °C for future use. We used NEBNext Ultra II DNA Library Prep Kit for
418 Illumina (New England Biolabs, NEB) and followed the manufacturer’s
419 manual with several exceptions:

420 1. ligation time was increased to 1 hour, 5 μ M adapter complex
421 was diluted with adapter dilution buffer (10 mM Tris-HCl, 1 mM
422 EDTA, 10 mM NaCl, pH 8) to 500 nM before use and replaced NEB
423 adapter,

424 2. 3 μ L of 5'-deadenylase (NEB) were added to ligation reaction,
425 3. strand displacing extension (sample 40 μ L, 10x buffer 10 μ L,
426 0.2 mM dNTP, polymerase 1 μ L, H₂O up to 100 μ L) was performed
427 with phi29 DNA polymerase (New England Biolabs) at 30 °C for
428 20 minutes, followed by standard AMPure XP (Beckman Coulter)
429 clean up with 0.75x volume ratio,

430 4. KAPA HiFi HotStart ReadyMix and xGen Library Ampli-
431 fication Primer Mix (IDT) were used for PCR by following the
432 manufacturer’s manuals with 2 minutes of extension,

433 5. and AMPure XP clean up with 0.75x volume ratio was per-
434 formed twice after the PCR.

435 Libraries for standard NGS and Duplex Sequencing were prepared
436 as described elsewhere[24]. All Library preparations were performed on
437 twin.tec PCR Plates LoBind 250 μ L (Eppendorf). Library quantitation
438 was performed with Qubit dsDNA HS kit (Invitrogen) paired with
439 Bioanalyzer DNA High Sensitivity chips (Agilent).

440 **Enrichment.** Both pan-cancer and WES enrichment was performed
441 with xGen Hybridization and Wash kits and xGen Blocking Oligos
442 (IDT), following the manufacturer’s manual. For capture probes, xGen
443 Pan-cancer Panel (IDT, 800 kb) and custom WES panel for the Broad
444 Institute by Twist Bioscience were used.

445 **Sequencing.** Standard NGS and Duplex Sequencing were performed
446 with Illumina HiSeq 2500 Rapid Run (300 cycles) for a pan-cancer panel
447 and WGS. CODEC was performed with Illumina HiSeq 2500 Rapid
448 Run (500 cycles) for a pan-cancer panel and WGS, and NovaSeq SP
449 (500 cycles) for WGS and WES. The extra cycles were used to confirm
450 the CODEC structure.

451 **CODEC data processing.** Due to the unique CODEC
452 read structure, we developed CODECsuite (available at
453 <https://github.com/broadinstitute/CODECsuite>) to process CODEC
454 data (**Supplementary Note**). CODECsuite is written in C++14 and
455 python3.7 and we use snakemake6.0.3[42] as the workflow management
456 system. CODECsuite consists of 4 major steps: demultiplexing, adapter
457 trimming, consensus calling and computing accuracy. The first 3
458 steps are specific to CODEC data. The workflow also involves other
459 standard tools such as BWA[43], Fgbio and GATK[44]. Illumina
460 bcl2fastq was used to generate fastq files (with -R -, no -sample-sheet
461 because CODECsuite will demultiplex), but is not included in the
462 suite. To speed up the data processing, we recommend splitting the
463 fastq files in batches and processing them in parallel. In this study,
464 using 40 batches, the preprocessing (demultiplexing and adapter
465 trimming) of 800M NovaSeq reads took just a few hours in a HPC
466 environment where each batch was executed using a single CPU and 8G
467 RAM. After demultiplexing and adapter removal, we mapped the raw
468 reads using BWA(0.7.17-r1188) against human reference hg19. Fgbio
469 (<https://github.com/fulcrumgenomics/fgbio>) was then used to collapse
470 the PCR duplicates and to form essentially single-strand consensus
471 (SSC) reads. These SSC reads were then mapped to the reference
472 genome using BWA again. Next, the duplex consensus reads between
473 R1 and R2 were generated from the SSC alignments. We filtered a
474 consensus base if any of the bases from R1 or R2 has base quality less
475 than 30. The duplex consensus reads were aligned to the reference
476 genome using BWA and the subsequent alignments were indel realigned
477 using GATK3 (<https://hub.docker.com/r/broadinstitute/gatk3>).

478 **Duplex Sequencing data processing.** Duplex Sequencing data
479 processing used in this study has been described elsewhere[24, 38].
480 Briefly, Fgbio was used to generate duplex consensus and to filter the
481 consensus reads. The entire workflow and more details are available
482 at the CODECsuite github. Read families with at least 2 copies of
483 each strand were required for generating duplex consensus except for
484 Duplex Sequencing WGS, which relaxed the requirement to 1 copy of
485 each strand to get the best possible duplex recovery.

486 **Duplex recovery and downsample to certain family sizes.** Two
487 custom python scripts were used to generate Figure 2c and 2d, respec-
488 tively. For duplex recovery, we subsampled the pre-consensus family-

489 assigned reads (after Fgbio GroupReadsByUmi) per target at log spaced
490 fractions starting from 10^{-4} ($\text{np.logspace}(-4, 0, 30)$) and calculated the
491 number of duplex formed at each downsample fraction. In this study,
492 this allowed us to understand situations when only limited sequencing
493 was given (e.g., < 100 read pairs). To understand the impact of family
494 size on error rate, we wrote another python script for downsampling. In
495 our sample, the number of duplex consensus having the exact family
496 sizes (number of pre-collapsed raw reads) were limited and thus gave
497 less confident results. Thus, we took advantage of families with strictly
498 larger family sizes and downsample them to the target family size. We
499 also sought to maintain an equal or close ratio between the number of
500 reads from each strand.

501 **Error rates in capture sequencing.** Throughout the article, we
502 defined the error rate as substitution error rate at the base level after
503 mapping to the reference genome (hg19). We used the substitution error
504 rate for calculating the general error rates because Illumina sequencers
505 usually generate 100-fold less indel errors[45] and this definition is com-
506 pliant with what other studies have reported[30]. For panel sequencing
507 with match normal, we used [Miredas](#) to calculate the error rate in
508 concordance with our previous work[24]. The duplex BAMs from both
509 cfDNA and matched normal samples were generated in the same way
510 and were applied to the same set of filters: 1. no secondary and supple-
511 mentary alignments; 2. Mapq ≥ 60 ; 3. Levenshtein distance (L-distance)
512 between the reads excluding soft clipping and reference genome ≤ 5 and
513 number of non N-base L-distance ≤ 2 ; 4. Excluding bases within 12 bp
514 distance from both fragment ends. In order not to confuse errors with
515 real mutations, we pre-computed the germline SNVs and using GATK4
516 (HaplotypeCaller[46]) from the Duplex Sequencing normal samples as
517 they have higher on-target ratio and hence coverage (89% vs 40% of
518 CODEC). For the patient sample, we found three somatic SNVs (median
519 VAF=0.26, range 0.24 - 0.28) in the captured regions (**Supplementary**
520 **Table S3**) using MuTect[39]. Those somatic mutations (patient sample
521 only) and germline mutations were masked when calculating the error
522 rates. The error rates were only reported for cfDNA samples and the
523 match normal were used for filtering possible germline (failed to call
524 or did not pass quality filter by HaplotypeCaller) and CHIP. Thereby
525 we also masked any SNV positions where there were at least 1 duplex
526 read support in match normal samples as CHIP can occur at very low
527 mutation frequency. Finally, the specificity checks[24] were performed
528 on cfDNA samples to remove substitutions that may rise from alignment
529 errors.

530 **Error rate in whole genome sequencing.** The WGS error rate was
531 computed similarly to capture data, except for a few differences. 1, We
532 used 'codec accuracy', a C++ program, as a replacement for Miredas
533 due to its speed improvement. 2, We used v3.3.2 GIAB NA12878 high
534 confidence VCF and BED[35] file as germline masks and evaluation
535 regions. 3, there was no match normal. 4, we forwent specificity checks
536 as it is also very slow for large genomes.

537 **Germline SNV and small indel calling in downsampled WGS.**
538 We merged the HiSeq 2500 Rapid Run and NovaSeq SP CODEC data
539 to evaluate germline variant calling. The merged CODEC and standard
540 WGS NA12878 samples were downsampled to 1 to 10x (step size 1x)
541 median coverage in the high confidence regions using GATK Downsam-
542 pleSam. Next, we ran GATK4.1.4.1 best practices pipeline via Cromwell
543 and Terra workflow (available at [web resources](#)) and computed on the
544 Google Cloud Platform. We used RTG [vcfEval](#) to calculate False Pos-
545 itives (FP) and False Negatives (FN) for SNVs and indels (< 50 bp)
546 without penalizing genotyping error (if heterozygous variants are called
547 as homozygous and vice versa) using v3.3.2 high confidence VCF and
548 BED file as input. We then calculated FP per million bases by normal-
549 izing against the high confidence region size and FN ratio by dividing
550 FN by the total number of true variants.

551 **Microsatellite instability detection.** The full-coverage CODEC
552 consensus BAM and full-coverage standard NGS R1R2 consensus BAM
553 on NA12878 were compared against each other to demonstrate CODEC
554 ability to correct PCR stutter errors and thus to reduce background
555 noise for MSI detection. MSIsensor-pro[47] was used to scan the hg19
556 for homopolymers of size 8 - 18 nt. Since MSIsensor-pro does not have
557 mapping quality or secondary alignments filters, we pre-filtered the
558 BAM using SAMtools[48] by requiring mapq ≥ 60 and no secondary or
559 supplementary alignments. And then it was used again to count the
560 number of reads that support different lengths of homopolymer at those
561 pre-selected sites. We removed any homopolymer sites that overlap or

562 are in close proximity (+/-5 bp) with any germline variants. After that,
563 the reference lengths of the homopolymer sites were considered as true
564 lengths. And observed length distributions from reads were compared
565 against truth. The results were generated from chromosome 1 only.

566 **Code availability.** CODECsuite and examples and tutorials including
567 how to regenerate the figures in the manuscript are available at
568 the github site <https://github.com/broadinstitute/CODECsuite>.
569 The end-to-end workflow is available at
570 <https://github.com/broadinstitute/CODECsuite/tree/master/snakefile>.

571 **Data availability.** CODEC data and Duplex Sequencing data will be
572 available on dbGAP.
573

References

- [1] Lennon, A. M. et al. Feasibility of blood testing combined with PET-CT to screen for cancer and guide intervention. *Science* 369, eabb9601 (2020).
- [2] Deveson, I. W. et al. Evaluating the analytical validity of circulating tumor DNA sequencing assays for precision oncology. *Nat. Biotechnol.* (2021) doi:10.1038/s41587-021-00857-z.
- [3] Vasan, N., Baserga, J. & Hyman, D. M. A view on drug resistance in cancer. *Nature* 575, 299–309 (2019).
- [4] Beaubier, N. et al. Integrated genomic profiling expands clinical options for patients with cancer. *Nat. Biotechnol.* 37, 1351–1360 (2019).
- [5] Griffith, O. L. et al. The prognostic effects of somatic mutations in ER-positive breast cancer. *Nat. Commun.* 9, 3476 (2018).
- [6] Jamal-Hanjani, M. et al. Tracking the Evolution of Non-Small-Cell Lung Cancer. *N. Engl. J. Med.* 376, 2109–2121 (2017).
- [7] Gerlinger, M. et al. Intratumor Heterogeneity and Branched Evolution Revealed by Multiregion Sequencing. *N. Engl. J. Med.* 366, 883–892 (2012).
- [8] Gerstung, M. et al. The evolutionary history of 2,658 cancers. *Nature* 578, 122–128 (2020).
- [9] D'Gama, A. M. & Walsh, C. A. Somatic mosaicism and neurodevelopmental disease. *Nature Neuroscience* 21, 1504–1514 (2018).
- [10] Serra, E. G. et al. Somatic mosaicism and common genetic variation contribute to the risk of very-early-onset inflammatory bowel disease. *Nat. Commun.* 11, 995 (2020).
- [11] Blauwkamp, T. A. et al. Analytical and clinical validation of a microbial cell-free DNA sequencing test for infectious disease. *Nat. Microbiol.* 4, 663–674 (2019).
- [12] Ménard, D. et al. A Worldwide Map of *Plasmodium falciparum* K13-Propeller Polymorphisms. *N. Engl. J. Med.* 374, 2453–2464 (2016).
- [13] Brazhnik, K. et al. Single-cell analysis reveals different age-related somatic mutation profiles between stem and differentiated cells in human liver. *Sci. Adv.* 6, (2020).
- [14] Bick, A. G. et al. Inherited causes of clonal haematopoiesis in 97,691 whole genomes. *Nature* 586, 763–768 (2020).
- [15] Wenger, A. M. et al. Accurate circular consensus long-read sequencing improves variant detection and assembly of a human genome. *Nat. Biotechnol.* 37, 1155–1162 (2019).
- [16] Karst, S. M. et al. High-accuracy long-read amplicon sequences using unique molecular identifiers with Nanopore or PacBio sequencing. *Nat. Methods* 18, 165–169 (2021).
- [17] Shendure, J. et al. DNA sequencing at 40: past, present and future. *Nature* 550, 345–353 (2017).
- [18] Arbeithuber, B., Makova, K. D. & Tiemann-Boege, I. Artifactual mutations resulting from DNA lesions limit detection levels in ultrasensitive sequencing applications. *DNA Res.* 23, 547–559 (2016).
- [19] Potapov, V. & Ong, J. L. Examining Sources of Error in PCR by Single-Molecule Sequencing. *PLoS One* 12, 1–19 (2017).
- [20] Goodwin, S., McPherson, J. D. & McCombie, W. R. Coming of age: ten years of next-generation sequencing technologies. *Nat. Rev. Genet.* 17, 333–351 (2016).
- [21] Kinde, I., Wu, J., Papadopoulos, N., Kinzler, K. W. & Vogelstein, B. Detection and quantification of rare mutations with massively parallel sequencing. *Proc. Natl. Acad. Sci. U. S. A.* 108, 9530–9535 (2011).
- [22] Kivioja, T. et al. Counting absolute numbers of molecules using unique molecular identifiers. *Nat. Methods* 9, 72–74 (2012).
- [23] Schmitt, M. W. et al. Detection of ultra-rare mutations by next-generation sequencing. *Proc. Natl. Acad. Sci. U. S. A.* 109, 14508–14513 (2012).
- [24] Parsons, H. A. et al. Sensitive Detection of Minimal Residual Disease in Patients Treated for Early-Stage Breast Cancer. *Clin. cancer Res.* 26, 2556–2564 (2020).
- [25] Pel, J. et al. Duplex Proximity Sequencing (Pro-Seq): A method to improve DNA sequencing accuracy without the cost of molecular barcoding redundancy. *PLoS One* 13, 1–19 (2018).
- [26] Gregory, M. T. et al. Targeted single molecule mutation detection with massively parallel sequencing. *Nucleic Acids Res.* 44, e22 (2016).
- [27] Wang, K. et al. Ultrasensitive and high-efficiency screen of de novo low-frequency mutations by o2n-seq. *Nat. Commun.* 8, 15335 (2017).
- [28] Lou, D. I. et al. High-Throughput DNA sequencing errors are reduced

643 by orders of magnitude using Circle Sequencing. *Proc. Natl. Acad. Sci.* 682 [43] Li, H. & Durbin, R. Fast and accurate long-read alignment with
644 U. S. A. 110, 19872–19877 (2013). 683 Burrows-Wheeler transform. *Bioinformatics* 26, 589–595 (2010).
645 [29] Hoang, M. L. et al. Genome-wide quantification of rare somatic mu- 684 [44] DePristo, M. A. et al. A framework for variation discovery and geno-
646 tations in normal human tissues using massively parallel sequencing. 685 typing using next-generation DNA sequencing data. *Nat. Genet.* 43,
647 *Proc. Natl. Acad. Sci. U. S. A.* 113, 9846–9851 (2016). 686 491–498 (2011).
648 [30] Abascal, F. et al. Somatic mutation landscapes at single-molecule 687 [45] Schirmer, M. et al. Insight into biases and sequencing errors for amplicon
649 resolution. *Nature* 593, 405–410 (2021). 688 sequencing with the Illumina MiSeq platform. *Nucleic Acids Res.* 43,
650 [31] Kircher, M., Sawyer, S. & Meyer, M. Double indexing overcomes in- 689 e37 (2015).
651 accuracies in multiplex sequencing on the Illumina platform. *Nucleic 690 [46] DePristo, M. A. et al. A framework for variation discovery and geno-
652 Acids Res.* 40, e3–e3 (2012). 691 typing using next-generation DNA sequencing data. *Nat. Genet.* 43,
653 [32] Costello, M. et al. Characterization and remediation of sample index 692 491–498 (2011).
654 swaps by non-redundant dual indexing on massively parallel sequencing 693 [47] Jia, P. et al. MSIsensor-pro: Fast, Accurate, and Matched-normal-
655 platforms. *BMC Genomics* 19, 332 (2018). 694 sample-free Detection of Microsatellite Instability. *Genomics. Proteomics* 695
656 [33] Xiong, K. et al. Duplex-Repair enables highly accurate sequencing, 696 *Bioinformatics* 18, 65–71 (2020).
657 despite DNA damage. *bioRxiv* (2021) doi:10.1101/2021.05.21.445162.
658 [34] Kim, S. et al. Deamination Effects in Formalin-Fixed, Paraffin- 697 [48] Li, H. et al. The Sequence Alignment/Map format and SAMtools. 698
659 Embedded Tissue Samples in the Era of Precision Medicine. *J. Mol. 699 *Bioinformatics* 25, 2078–2079 (2009).
660 Diagnostics* 19, 137–146 (2017).
661 [35] Zook, J. M. et al. An open resource for accurately benchmarking small 699
662 variant and reference calls. *Nat. Biotechnol.* 37, 561–566 (2019).
663 [36] Yu, F. et al. NGS-based identification and tracing of microsatellite 700
664 instability from minute amounts DNA using inter-Alu-PCR. *Nucleic 701
665 Acids Res.* 49, e24–e24 (2021).
666 [37] Woodworth, M. B., Girsikis, K. M. & Walsh, C. A. Building a lineage 702
667 from single cells: Genetic techniques for cell lineage tracking. *Nat. Rev. 703
668 Genet.* 18, 230–244 (2017).
669 [38] Gydush, G. et al. MAESTRO affords ‘breadth and depth’ for mutation 704
670 testing. *bioRxiv* (2021) doi:10.1101/2021.01.22.427323.
671 [39] Cibulskis, K. et al. Sensitive detection of somatic point mutations in 705
672 impure and heterogeneous cancer samples. *Nat. Biotechnol.* 31, 213–219 706
673 (2013).
674 [40] May, A., Abeln, S., Crielaard, W., Heringa, J. & Brandt, B. W. Un- 707
675 raveling the outcome of 16S rDNA-based taxonomy analysis through 708
676 mock data and simulations. *Bioinformatics* 30, 1530–1538 (2014).
677 [41] Limasset, A., Flot, J. F. & Peterlongo, P. Toward perfect reads: Self- 709
678 correction of short reads via mapping on de Bruijn graphs. *Bioinfor- 710
679 matics* 36, 1374–1381 (2020).
680 [42] Mölder, F. et al. Sustainable data analysis with Snakemake. 711
681 *F1000Research* 10, 33 (2021).
712

698 Acknowledgements

699 The authors acknowledge the Gerstner Family Foundation for its
700 generous support. This study was also supported in part by SPARC
701 award from the Broad Institute.

702 Author contributions

703 Conception and design: V.A.A., J.H.B.
704 Method development: V.A.A., J.H.B., R.L.
705 Data acquisition: J.H.B., E.N.
706 Data analysis: R.L.
707 Data interpretation: V.A.A., Z.A., J.H.B., T.B., G.G., R.L., E.N.,
708 S.P., J.R. D.S., S.T., K.X.
709 Writing and review of the manuscript: V.A.A., J.H.B., T.R.G., R.L.,
710 G.M.M.

711 Competing interests

712 The authors have filed a patent application on this method. V.A.A. is
713 a member of the scientific advisory boards of AGCT GmbH and Bertis
714 Inc. T.R.G. has advisor roles at Foundation Medicine, GlaxoSmithKline,
715 and Sherlock Biosciences.